Supplementary information

In Situ Solid−Gas Reactivity of Nanoscaled Metal Borides from Molten Salt Synthesis

*Guillaume Gouget[a], Damien P. Debecker[b], Ara Kim[a,b], Giorgia Olivieri[c], Jean-Jacques Gallet[c,d], Fabrice Bournel[c,d], Cyril Thomas[e], Ovidiu Ersen[f], Simona Moldovan,[f], Clément Sanchez[a], Sophie Carenco[a] and David Portehault[a]**

[a] Sorbonne Universités-UPMC Univ. Paris 06, CNRS, Collège de France, Laboratoire de Chimie de la Matière Condensée de Paris, 4 place Jussieu, F-75252 Paris Cedex 05, France.

[b] Université catholique de Louvain, Institute of Condensed Matter & Nanosciences, Molecules, Solids & Reactivity, Place Louis Pasteur 1, 1348 Louvain-la-Neuve, Belgium.

[c] Synchrotron SOLEIL, L'Orme des Merisiers, Saint-Aubin, BP 48, 91192 Gif sur Yvette Cedex, France.

[d] Sorbonne Universités, UPMC Univ Paris 06, Laboratoire de Chimie Physique, Matière et Rayonnement, 4 place Jussieu, F-75252 Paris Cedex 05, France.

[e] Sorbonne Universités, UPMC Univ. Paris 06, CNRS, Laboratoire de Réactivité de Surface, 4 place Jussieu, F-75252 Paris Cedex 05, France.

[f] Institut de Physique et Chimie des Matériaux de Strasbourg, CNRS, 23 Rue Loess, BP 43, F-67034 Strasbourg, France.

Methods

Figure S1. *In situ* TEM analysis of the CoB nanocomposite under (a) 0.3 bar of argon at 150 °C, and (b) 0.9 bar of H_2 at 400 °C.

Figure S2. XPS surveys of the CoB nanocomposite at various steps of the *in situ* study.

Figure S3. Methane production rate as a function of temperature for various samples after 20 min on stream.

Figure S4. XRD diagrams of CoB supported on TiO_2 at different steps of the methanation.

Figure S5. CH_4 production rate as a function of time on stream for SiO_2- and TiO_2-supported CoB at 400 and 500 °C.

Figure S6. Powder XRD patterns of the CoB nanocomposite supported on SiO_2 before exposure to the reducing treatment and after different steps of the catalytic process.

Figure S7. Powder XRD patterns of CoB nanoparticles before and after heat treatment under H_2:Ar (5:95 volume ratio).

Techniques

Powder X-ray diffraction (XRD). XRD measurements were performed on a D8 Bruker apparatus operating at the Cu-Kα radiation. Patterns were indexed according to ICDD files: CoB (04-003-2122), cubic Co (04-001-2681), hexagonal Co (04-01-3273), Co_3O_4 (04-05-4386), NiB (01-074-1207), Ni_4B_3 (01-073-2551), Ni_3B (04-014-0853) and Ni (04-010-6148). Apparent crystallite sizes were calculated using the Scherrer formula and pseudo-Voigt functions to fit peaks. The samples after the pretreatments and the catalytic reactions were extracted and analyzed by XRD in inert atmosphere using a glovebag filled with nitrogen and a protective sample holder.

Transmission electron microscopy (TEM). A 120 kV Tecnai Spirit microscope was used for TEM. High Resolution-TEM (HRTEM) was also operated on a 200 kV JEOL JEM 2011 apparatus, at the Institut des Matériaux de Paris Centre (IMPC). Samples were prepared by evaporating a drop of suspension in ethanol on a carbon-coated copper grid. SAED pictures were calibrated with gold nanoparticles.

Energy Dispersive X-Ray spectrometry (EDX). Elemental EDX analyses were obtained on a Scanning Electron Microscope (SEM) S-3400-N (Hitachi) equipped with an EDX detector (Oxford) calibrated prior measurements to allow retrieving quantitative data. 100 x 50 μm^2 areas were probed. Acceleration tension of the source was 10 kV. A titanium grid was used for quantitative calibration. The samples were fixed to a conductive carbon tape.

Inductive coupled plasma-Optical Emission Spectrometry. ICP-OES measurements were acquired on an iCAP 6000 apparatus (ThermoFischer). The sample was prepared by dissolving the cobalt boride powder in a 5 mol L^{-1} nitric acid solution followed by a 10 times dilution in deionized water. Each concentration is the average of three measurements.

Nitrogen sorption. Samples were degassed at 150 °C overnight before measuring on an ASAP 2000 apparatus (Micromeritics).

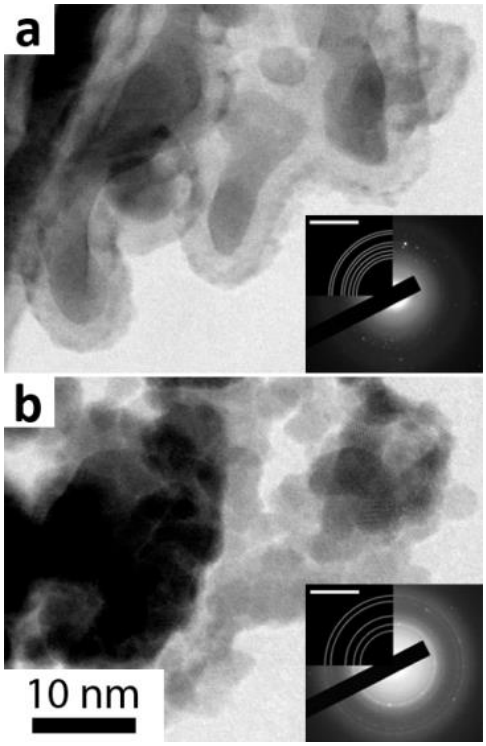

Figure S1. *In situ* TEM analysis of the CoB nanocomposite under (a) 0.3 bar of argon at 150 °C, and (b) 0.9 bar of H_2 at 400 °C. The SAED patterns are indexed (a) along the CoB structure and (b) along the Co_3O_4 structure. Note that the surprising occurrence of Co_3O_4, contrary to UHV-XPS, NAP-XPS and *ex situ* XRD, arises from the very small gas flow and non-optimized gas inlet used in this apparatus, which likely resulted in traces of oxygen impurities in the flow.

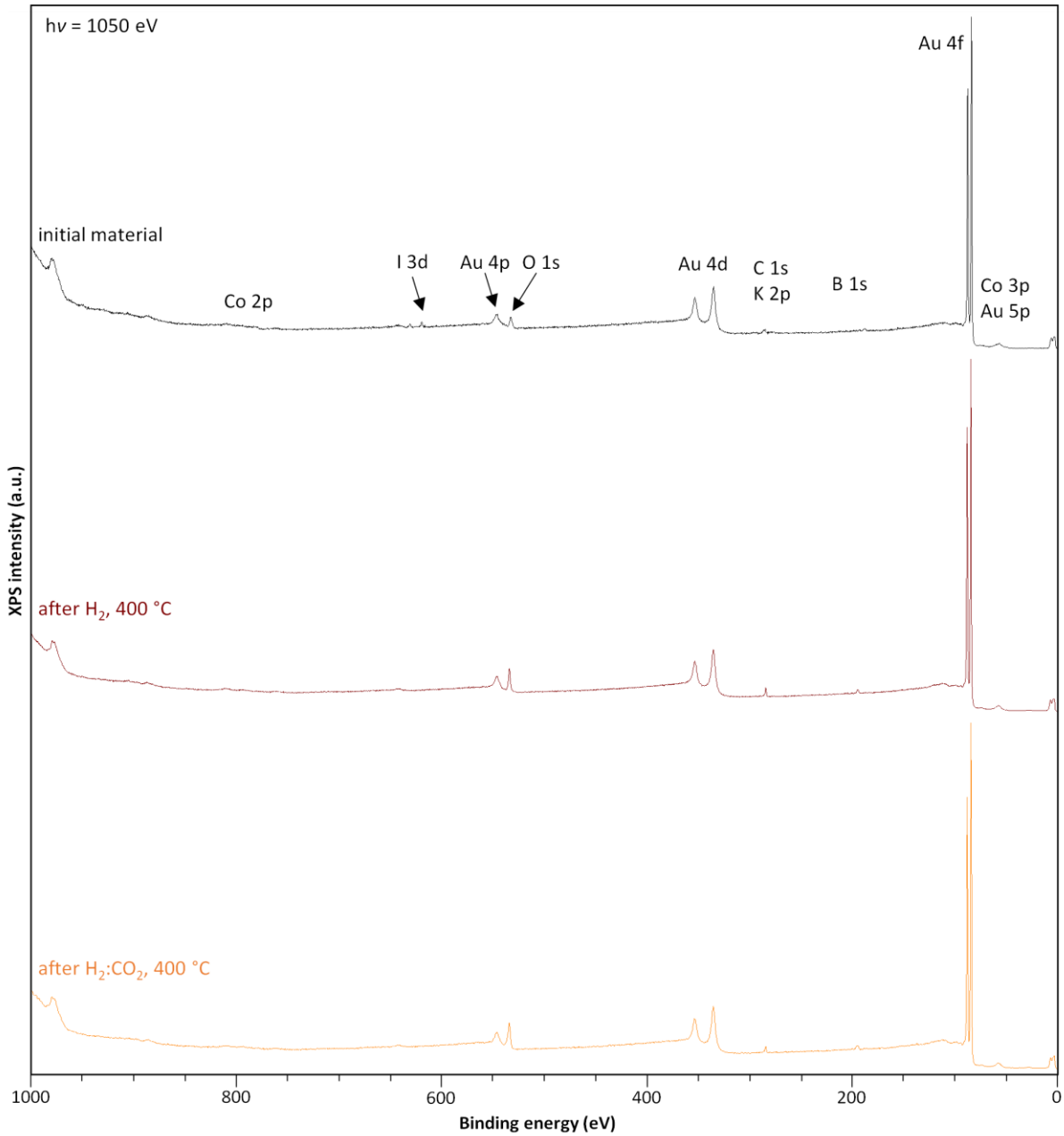

Figure S2. UHV-XPS surveys of the initial CoB nanocomposite (black), after exposure to 1 bar of H_2 at 400 °C in UHV (maroon) and after exposition to H_2:CO_2 (4:1 vol., orange) at 400 °C. *hν*: photon energy. Potassium and iodine are detected only in the initial material. These impurities come from the inorganic salt medium in which the nanocomposite is synthetized. These elements were not detected by SEM-EDX. They are thus present in very small proportion, are located only at the surface and eliminated during the first heat treatment.

Note that after NAP-XPS experiments and return to room temperature and UHV conditions, two other species are detected by XPS ("BO_x" on Figure 4 in the main text). Indeed, two oxygen contributions appear at 536.9 and 537.9 eV. In the B 1s region under UHV conditions, two peaks at 197.1 and 198.1 eV appear in addition to the BO_3 peak at 195.4 eV. The area ratios between the two oxygen peaks and

between the two boron peaks are identical. The four contributions are thus interlinked, with couples (O 1s, B 1s) attributed to two unusual fully oxidized boron species with binding energies that are much higher than any other reported previously.(M. M. Ennaceur, B. Terreault, XPS Study of the Process of Oxygen Gettering by Thin Films of PACVD Boron. *J. Nucl. Mater.* 2000, **280**, 33–38; B. R. Strohmeier, Surface Characterization Of Ammonium Fluoborate. 1989, **40**, 249–263)

When the material is heated again under NAP conditions (data not shown), these two species disappear and the NAP-XPS spectra are found similar to those shown in Figure 4, red spectra, thus indicating the reversibility of such structural changes under UHV conditions. These high-energy peaks may originate from locally distorted boron oxides only stable under UHV conditions. Similar phenomena have been described during the reduction of cerium oxides.(J. Holgado, G. Munuera, J. Espinós, A. González-Elipe, XPS Study of Oxidation Processes of CeO_x Defective Layers. *Appl. Surf. Sci.* 2000, **158**, 164–171) These UHV metastable species are not representative of the material exposed to environmental conditions and have not been further investigated.

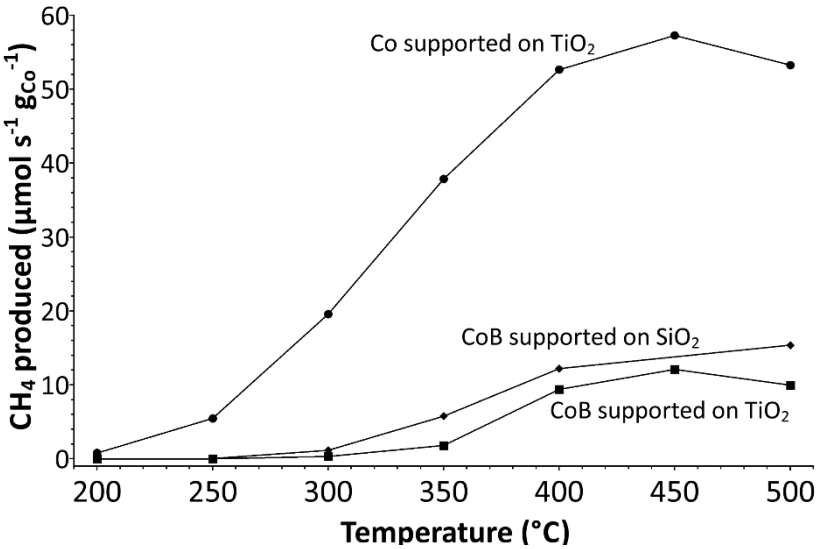

Figure S3. Methane production rate as a function of temperature for various samples after 20 min on stream. Supported CoB were treated under H_2 (1 atm, 30 mL min^{-1}) at 400 °C. The reactive gas mixture during the methanation reaction was CO_2:H_2:He (vol. ratio 1:4:5, 1 atm, 20 mL min^{-1}).

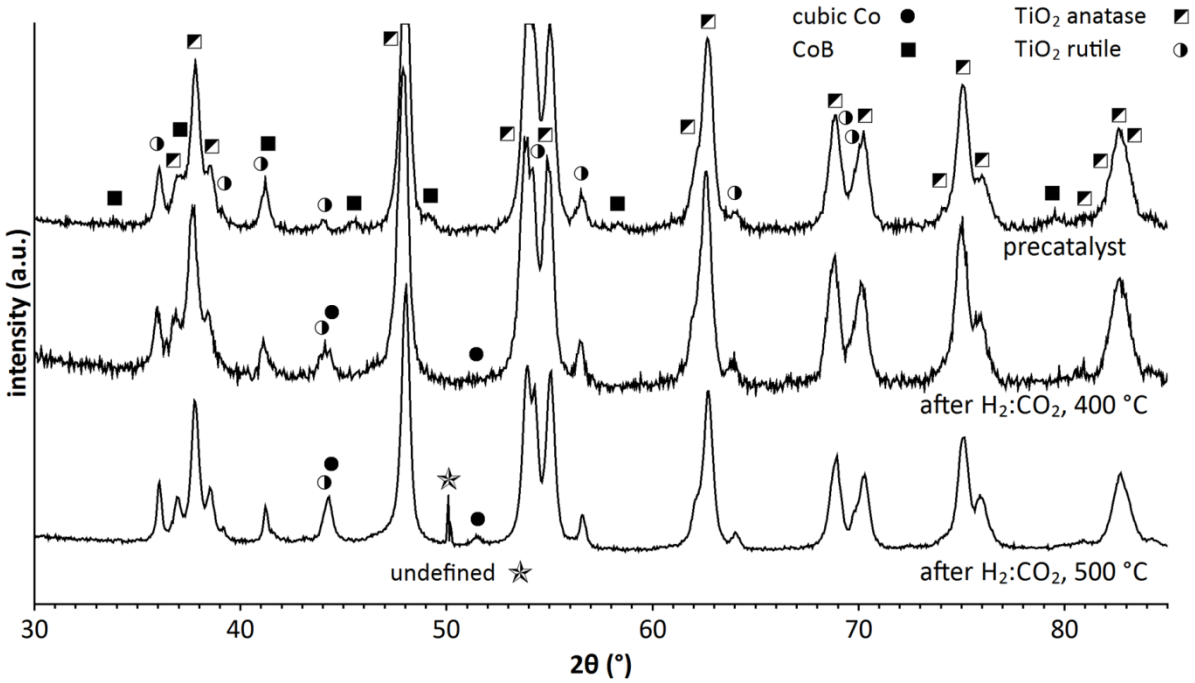

Figure S4. XRD patterns of CoB supported on TiO_2 at different steps. The anatase and rutile phases of TiO_2 are indexed according to the ICDD files 00-021-1272 and 00-021-1276, respectively.

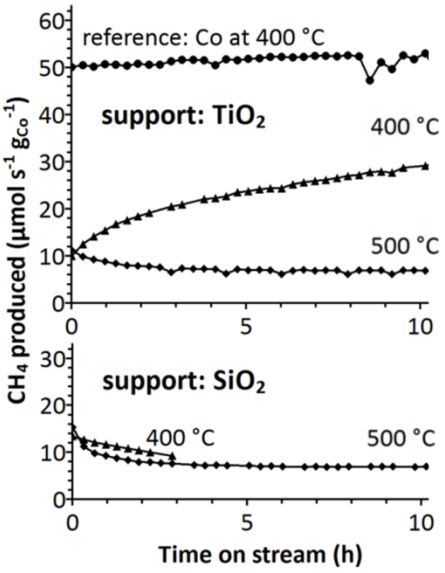

Figure S5. CH_4 production rate as a function of time on stream for SiO_2- and TiO_2-supported CoB at 400 and 500 °C. The behavior of a Co/TiO_2 reference sample is also shown for comparison. Inner gas mix: H_2:CO_2:He (4:1:5 vol.), 1 atm, 20 mL min^{-1}. Pretreatment: H_2, 1 atm, 30 mL min^{-1} at 400 °C for 2 h. For CoB supported on SiO_2, the CH_4 production rate decreases upon time on stream, leading to a 2-fold decrease at 500 °C within 2 h on stream. Then the rate reaches steady state at around 7 mol s^{-1} g_{Co}^{-1}.

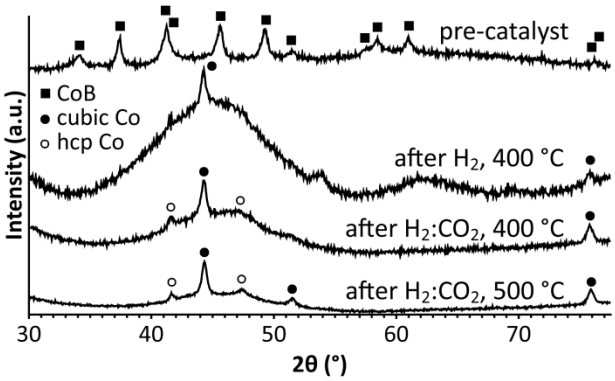

Figure S6. Powder XRD patterns of the CoB nanocomposite supported on SiO_2 before exposure to the reducing treatment and after different steps of the catalytic process. In the initial state, the XRD pattern is similar to that recorded for the unsupported material (Figure 1a in the main text), with broad peaks corresponding to CoB nanoparticles and crystallite sizes of 14±3 nm according to the Scherrer formula. After exposure to H_2 at 400 °C for 2 h, CoB reflections disappear, whereas peaks corresponding to cubic Co are detected, in agreement with UHV-XPS and NEXAFS data, with an apparent diameter of 18±4 nm. A broad contribution to the baseline is observed in addition to crystalline Co, indicating that the amorphous part of the material has evolved compared to the pre-catalyst. After exposure to the methanation conditions at 400 °C for 3 h, metallic cobalt is also observed in the cubic and hexagonal structures with a crystallite size of 15±2 nm. After methanation at 500 °C, the presence of cubic and hexagonal Co crystallites is also identified with the same apparent size.

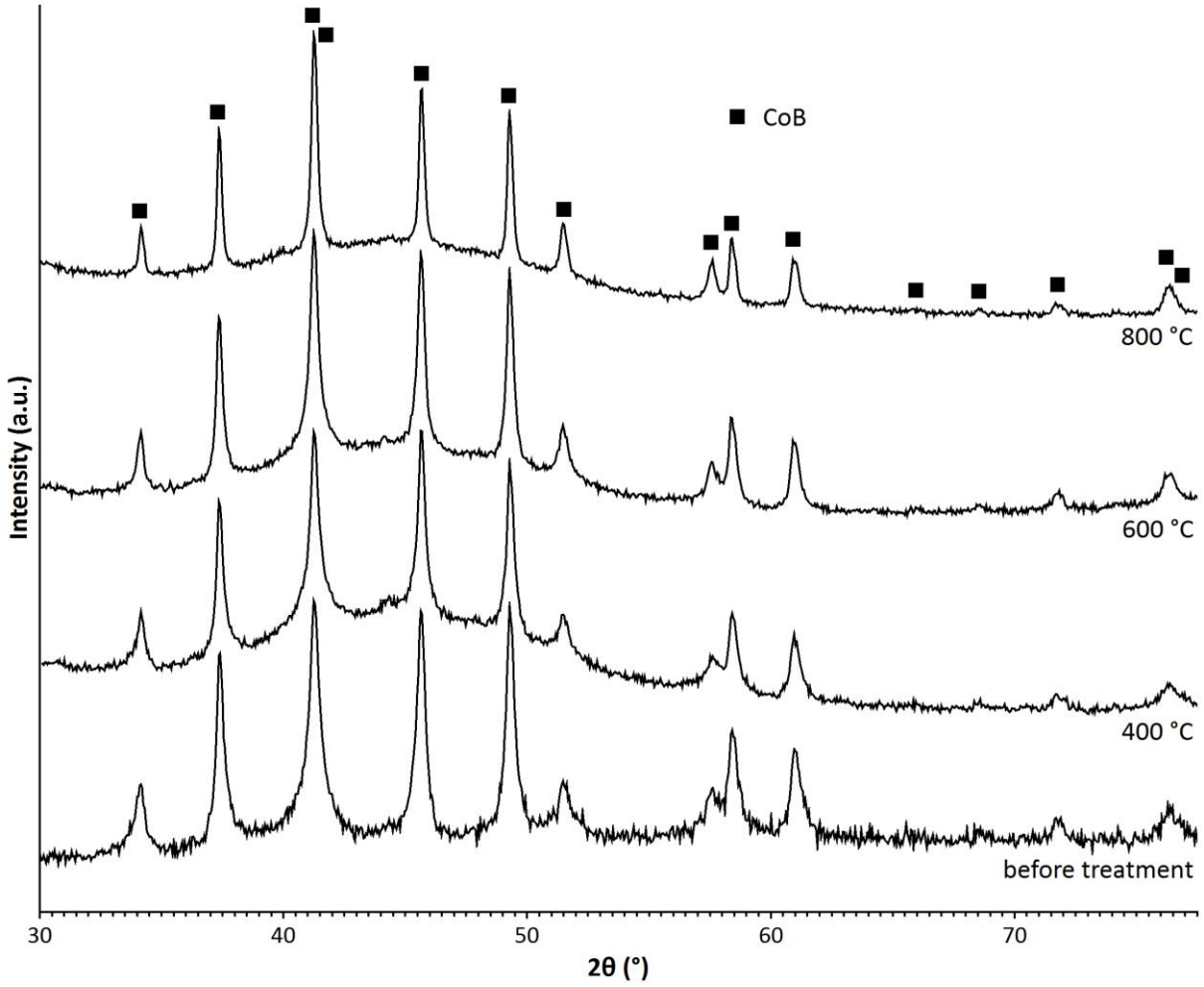

Figure S7. Powder XRD patterns of CoB nanoparticles before and after heat treatment under H_2:Ar (5:95 volume ratio) at various temperatures for 2 h. Heat treatments in a mix of argon and dihydrogen (5 %) do not lead to cobalt boride decomposition. CoB remains the only crystalline phase detected, even after heating at 800 °C. Reflections sharpen with increasing temperature due to nanocrystal growth.